ELSEVIER

Ultrasonics 39 (2001) 263–268

Ultrasonics

www.elsevier.nl/locate/ultras

Propagation speed of sound assessment in the layers of the guinea-pig esophagus in vitro by means of acoustic microscopy

J.E. Assentoft [a], H. Gregersen [a,b], W.D. O'Brien Jr. [c,*]

[a] *Institute of Experimental Clinical Research, Skejby Hospital, Section SKS, Denmark*
[b] *Center for Sensory-Motor Interaction, Aalborg University and Department A, Aalborg Hospital, Denmark*
[c] *Department of Electrical and Computer Engineering, Bioacoustics Research Laboratory, University of Illinois at Urbana-Champaign, 405 N. Mathews, Urbana, IL 61801, USA*

Received 11 August 2000; received in revised form 18 December 2000; accepted 21 December 2000

Abstract

The study's purpose was to evaluate the propagation speed of sound in the tissue layers of the esophagus at various mechanical loadings. Scanning laser acoustics microscopy was applied for the estimation of the propagation speed in the mucosa–submucosa and muscle layers of guinea-pig esophagus in vitro ($n = 26$). The propagation speed in the esophagus was determined in the no-load state with all external forces removed, and in the distended and zero-stress states. The zero-stress state was obtained by cutting the esophageal rings radially. The propagation speed in the no-load state differed significantly ($p < 0.001$) between the muscle layer (median 1740, quartiles 1735–1746 m/s) and the mucosa (1607, 1605–1609 m/s). In the distended state the propagation speed in the muscle layer decreased significantly ($p < 0.001$) to 1673 (1666–1681) m/s while it did not change significantly in mucosa (1602, 1600–1607 m/s). When compared to the no-load state, the propagation speed in the zero-stress state in the muscle layers decreased to 1624 (1615–1636) m/s ($p < 0.001$) and in mucosa to 1584 (1566–1603) m/s ($p < 0.001$). In conclusion, the esophagus is a composite structure with heterogeneous propagation speed characteristics. Furthermore, the mechanical loading state must be considered in esophageal ultrasound studies.

Keywords: Ultrasound propagation speed; Mucosa; Muscle; Digestive tract

1. Introduction

The advancement of science in recent years follows a trend of needing to know greater details in physiology, medicine and tissue engineering. Obtaining morphometric and biomechanical data from several adjacent layers of tissue is a step towards the next level in the hierarchy of structure of living tissue. Such data are needed in a mechanical analysis of a composite biological structure. Thus far, Yu et al. [1] presented a two-layer model based on bending experiments for determination of stress–strain properties. Gregersen et al. [2] studied the zero-stress state of the layers of guinea-pig esophagus and found significant differences in residual strain between the muscle and mucosa–submucosa layers. Realizing that obtaining mechanical data on individual layers of biological tissues are useful, we need to develop new methods to characterize layered organs to a greater extent. In this study we employed a scanning laser acoustic microscope (SLAM) to obtain a better understanding of the composite properties of the esophagus.

The practical application of ultrasound for imaging was demonstrated by the French physicist Paul Langevin during World War I [3]. In the early 1930s Sokolov explored the usefulness of ultrasound for imaging internal structures in optically opaque objects [3,4] and he was first to suggest ultrasound at 3 GHz for imaging small objects. This technique is now known as *acoustic microscopy*, which is defined as a general term for high resolution, high frequency ultrasonic inspection techniques that produce images of features beneath the surface of the sample. Further developments led to the SLAM which was introduced by Korpel and coworkers [5]. The SLAM is a transmission mode instrument that creates real-time acoustic images of a sample throughout its entire thickness. A collimated continuous-wave ultrasound beam at frequencies from 10 to 500 MHz is

* Corresponding author. Tel.: +1-217-333-2407; fax: +1-217-244-0105.
E-mail address: wdo@uiuc.edu (W.D. O'Brien Jr.).

0041-624X/01/$ - see front matter
PII: S0041-624X(01)00053-1

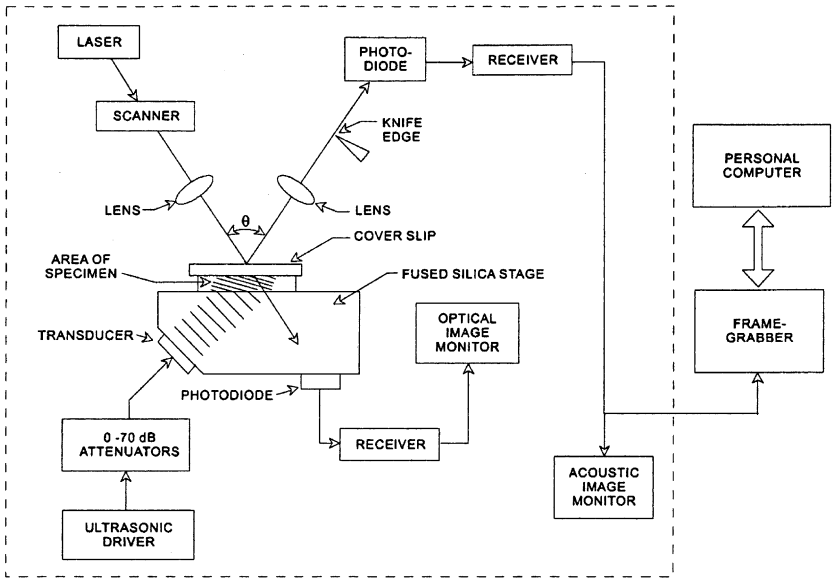

Fig. 1. Block diagram of the SLAM.

produced by a piezoelectric transducer located beneath the sample (for this study, 100 MHz was used). When the ultrasound wave propagates through the sample, the wave is affected by mechanical inhomogeneities in the material. A scanned laser beam is used as the ultrasound detector (Fig. 1). The ability of the SLAM to produce simultaneously optical and acoustic images from which the acoustic properties of the specimen can be calculated make easy its use in this field of biology. The ultrasonic attenuation and propagation speed can be estimated from the obtained information. Conventional tissue fixation and staining are not required for the SLAM imaging; this allows for studies of living cells and tissues [6]. The SLAM has been found useful for the in vitro assessment of acoustic properties in biological materials such as skin [7], kidney [8] and liver [9].

The SLAM technique was thus used as the method for estimating propagation speed in the simple layered structure of the guinea-pig esophagus. The esophagus consists of an innermost mucosa–submucosal layer (hereafter referred to as the mucosal layer) that mainly consists of connective tissue with blood vessels and nerves, and outermost longitudinal and circumferential muscle layers. The esophagus is an important organ to study due to its mechanical function and composite structure. Furthermore, diseases can cause structural and biomechanical remodeling in the esophagus.

The propagation speed in the individual layers of the esophagus has, to the best of our knowledge, not been presented in the literature. The aim of this study was to determine the propagation speed in the individual layers of esophagus in vitro in the no-load state with all external forces removed, in the distended state and in the zero-stress state. The distended state corresponds to the physiological state where a bolus of fluid or food passes through the esophagus. The no-load state is the conditions where no external forces are applied, i.e., zero pressure from outside and inside. The no-load state was for many years considered to be the reference state for mechanical analysis, i.e., the reference length for strain. However, we know now that residual stresses may reside in the no-load state. The cut-open state, also called the zero-stress state, is the condition where also the residual (internal) forces have been released by making a radial cut through the wall. The zero-stress state is important in mechanics because it is the state to where all the stresses and strains refer.

2. Material and methods

2.1. Specimen preparation

Twenty-six 700–900-g female guinea pigs were euthanized using pentobarbital, and a long midline cut was made in the neck and chest. Calcium-free Krebs solution was poured into the chest cavity. The esophagus was separated from adjacent structures from the tongue to the stomach. A 4-cm-long segment beginning 2 mm from the root of the tongue was excised. The tissue was cleaned and snap-frozen in one of four different states (see below) in liquid nitrogen and stored at −80°C.

At the time of sample evaluation, 100-μm-thick cross-sections were cut in a Lipshaw cryo-microtome. Each specimen was placed on the SLAM stage and allowed 5 min for equilibration to 24.5°C (as measured by an Omega Engineering Inc., Model HH21) before estimates of the propagation speed were performed. A physio-

logical saline solution was used as coupling medium between the SLAM stage and specimen and served as a reference medium (known acoustic properties) for calculation of the propagation speed. The experimental protocol was approved by the University of Illinois' Laboratory Animal Care Advisory Committee and satisfied all campus and National Institutes of Health (NIH) rules for the humane use of laboratory animals.

The esophagus was studied under four different conditions: distended state ($n = 26$), no-load state ($n = 26$), zero-stress state ($n = 26$) and finally the mucosal layer without the muscle layer attached ($n = 6$). The distended state corresponds to the homeostatic state with a food bolus in the esophagus. The distended state was obtained by infusing Tissue Tek (OCT) in the esophagus to a diameter, D, corresponding to an approximate stretch ratio, $D_{\text{distended}}/D_{\text{no-load}}$, at the outer surface of 1.15 before it was snap frozen. The stretch ratio did not change after mounting the specimen on the SLAM stage. The no-load state represents the condition without any external forces applied. The zero-stress state represents the state where residual stresses are not present, and was obtained by a radial cut that caused the esophagus to spring open. About thirty seconds after the radial cut, the sample was snap-frozen. The mucosal layer was studied under no-load conditions by removing the muscle layer surgically under a microscope before it was snap-frozen. Separation was performed without visible damage to the mucosal tissue; optical microscope magnification of 4× was used. The muscle layer was not suitable for investigation after separation.

2.2. Scanning laser acoustic microscopy

The technical details and operating principles of the SLAM (Sonomicroscope®, Sonoscan, Inc., Bensenville, Illinois) have previously been described in detail [10]. The three SLAM modes produce three different images. For all modes, the sample is located between the SLAM stage and plastic coverslip (Fig. 1). The coverslip is coated with a partially reflecting optical layer, and that layer is adjacent to the sample. In the *optical mode*, a focused laser beam scans the specimen from above, and is transmitted through the coverslip and specimen to a photodiode at the base of the stage. The received photodiode signal is electronically processed and displayed to a TV-monitor; the SLAM's optical image is comparable to that of conventional optical microscopy at a magnification of 100×, but is not comparable in that the light source is that of a laser. In the *acoustic mode*, the specimen is insonified with a 100-MHz (in this case) ultrasonic wave generated by a piezoelectric transducer located below the specimen. The sound wave traverses the specimen and is incident on the lower surface of the coverslip, the surface with the coating. The acoustic generated deflections on this surface of the coverslip are scanned by the laser beam that in turn is reflected to a photodiode. The laser signal is then processed into an acoustic-mode image and displayed in real time on the TV monitor. The ultrasonic attenuation of the specimen can be calculated from this acoustic image [11]. However, specimen attenuation was not possible for this experiment because the attenuation technique requires different thicknesses of the same sample, and there was insufficient sample material. In the *interference mode*, the laser beam is detected by the same photodiode as in the acoustic mode and it is then mixed with a 100-MHz reference signal to produce an interference image displayed on the TV-monitor (Fig. 2). From the interference image, the acoustic propagation speed is calculated from the lateral (horizontal) shift of the vertical interference lines [12]. The lines shift to the right when the sound waves enter an object having a higher speed relative to the coupling reference medium. Quantitative speed profiles (Figs. 3 and 4) are created from analysis of several image regions in different loci. The propagation speed of the specimen is calculated in relation to that of the 1520-m/s reference medium (calcium-free Krebs–Ringer solution with 10^{-2} M $MgCl_2$), hereafter referred to as the Krebs–Ringer solution, according to the following expression [12,13]:

$$C_x = \frac{C_o}{\sin\theta_o}\left[\tan^{-1}\left(\frac{1}{\frac{1}{\tan\theta_o} - \frac{\lambda_o N}{T\sin\theta_o}}\right)\right] \text{ m/s} \qquad (1)$$

where C_x is the propagation speed in the specimen of interest, C_o is the propagation speed in the reference

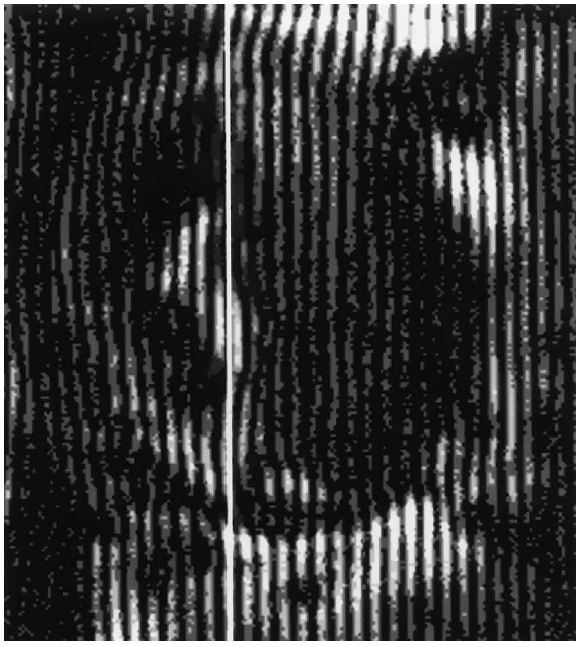

Fig. 2. An interference image of the cross-section of an esophagus. The darker vertical lines are the interference lines. The white vertical line that passes through the center of the esophagus indicates where the propagation speed profile was obtained that is displayed in Fig. 3.

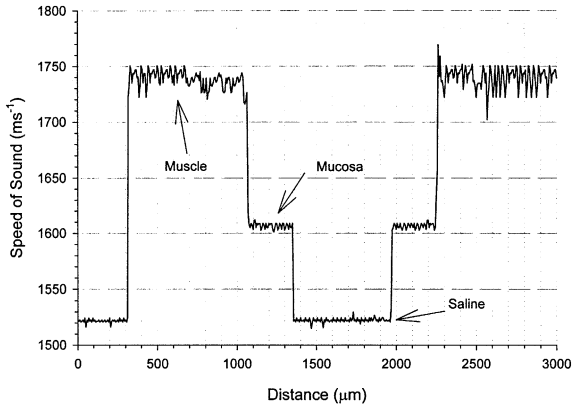

Fig. 3. The propagation speed profile that depicts the speed of muscle and mucosa layers in esophagus at no-load state. The distance axis goes from top to bottom (see vertical white line in Fig. 3) of the interference image. The reference medium is Krebs–Ringer solution.

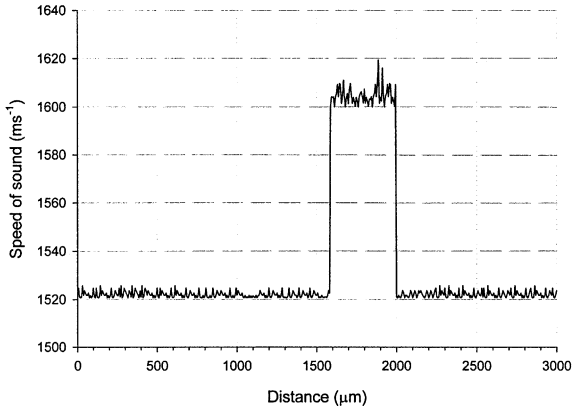

Fig. 4. The propagation speed profile in the mucosa layer of esophagus at the no-load state. The reference medium is Krebs–Ringer solution.

medium (Krebs–Ringer solution, 30°C, 1520 m/s), λ_o is the wavelength of sound in the reference medium, T is the specimen thickness, N is the measured normalized lateral fringe shift, θ_o is the angle between the direction of sound propagation in the reference medium and the normal to the stage surface, and is determined from Snell's law:

$$\theta_o = \sin^{-1}\left[\frac{C_o}{C_s}\sin\theta_s\right] \quad (2)$$

where C_s is the propagation speed in the fused silica stage (5968 m/s), and θ_s is the angle the sound wave travels through the stage (45°). Measurements of the propagation speed were done along the vertical line in each layer of the wall (Fig. 2) to yield a speed profile (Fig. 4).

2.3. Uncertainty of SLAM measurements

An uncertainty assessment of the SLAM's measurement procedures and results was performed by measuring the propagation speed in a known media (Dow Corning 710, Dow Corning, Midland, MI), a silicone oil for which attenuation coefficient and speed have been characterized acoustically and referenced in the literature [12,14,15]. A droplet of the oil was placed inside a metal spacer surrounded by saline on the scanning stage surface and a coverslip was then placed on top of the metal spacer. The thickness of the metal spacer was measured with a calibrated digital caliper to within ±1 μm. The saline and the oil did not mix. The oil was then allowed to equilibrate to 30°C before the measurement were taken. The propagation speed was determined for varying oil thickness (75 and 120 μm) with all other factors kept constant. Our experiments on Dow Corning 710 gave a propagation speed of 1341 m/s (quartiles 1321–1357 m/s). Hence, the precision was 2.7% $[((1357-1321)/1341)\times 100\%]$. For accuracy determination the median value of 1341 should be compared to values in the literature of approximately 1350 m/s [14]. Sources of speed error of the Dow Corning 710 included the reference medium speed (Krebs–Ringer solution), the normalized fringe shift, the specimen thickness, noise and other unknown variations in the SLAM system. Krebs–Ringer solution was used as the reference medium, and the temperature was kept stable to reduce the error due to the reference speed. The difference in propagation speed between thicknesses of 75 and 120 μm was less than 10 m/s. An extensive error analysis of SLAM measurements is provided by Steiger et al. [7].

Data are presented as median and quartiles. Statistical test was the Mann–Whitney Rank Sum test using SigmaStat (Jandel Scientific). Results were considered significant when $p < 0.05$.

3. Results

The propagation speed from the different layers and preparations are given in Table 1. It was not possible to distinguish the circular and longitudinal muscle layers in any of the preparations, though the sound beam direction was parallel to the longitudinal muscle layer and perpendicular to the circumferential muscle layer. It was a general finding that the propagation speed was higher in the muscle layer than in mucosa ($p < 0.001$ for the distended, no-load and zero-stress states). The most pronounced difference in propagation speed between the layers was found in no-load state (approximately 8% difference, Fig. 3). The propagation speed in the muscle layer differed among the three states ($p < 0.001$) with the highest median value of 1740 m/s in no-load state. The lowest value was found in the zero-stress state (1624, 1615–1636 m/s). In mucosa the propagation speed also varied between the three states ($p < 0.001$) with the lowest values in zero-stress state (1584, 1566–1603 m/s). The propagation speed in the no-load state for mucosa

Table 1
Propagation speed in the different layers of esophagus measured at 100 MHz

	Esophagus						
	No-load state		Distended state		Zero-stress state		Separated layer
	Muscle	Mucosa	Muscle	Mucosa	Muscle	Mucosa	Mucosa
Median speed (m/s)	1740	1607	1673	1602	1624	1584	1606
Quartiles (m/s)	1735–1746	1605–1609	1666–1681	1600–1607	1615–1636	1566–1603	1602–1609

Muscle differed from mucosa at all three states ($p < 0.001$). The propagation speed for the muscle layer differed between the three states ($p < 0.001$). The propagation speed for the mucosa layer differed between the three state ($p < 0.001$) but the mucosa separated from the muscle layer (last column) did not differ from the mucosa with the muscle layer attached in no-load state.

separated from the muscle layer did not differ from that obtained in mucosa with muscle attached (Figs. 3 and 4, Table 1).

4. Discussion

In this paper we show that it is possible with SLAM to image sections of the guinea-pig esophagus and quantitatively distinguish its layered topography. As far as we know there are no other acoustic microscope studies that have investigated the layered structures in esophagus. The wall can be quantitatively characterized and its layers distinguished by use of the SLAM propagation speed profile. We aimed to study the properties at different states of mechanical loading. The distended state corresponds to the in vivo state with bolus passage. In the no-load state, the specimen is not exposed to any external forces but residual stresses may be present in the tissue. Such residual stresses are released by cutting the tissue radially to achieve the zero-stress state. The zero-stress state was first described in biological tissues in 1983 [16,17] and it provides a reference state for morphometric and mechanical analysis. Recently, it was found that the guinea-pig esophagus and duodenum exhibit large residual strains and that the residual strain reduces the stress concentration at the luminal surface during loading [2,18,19]. It is of interest to note from this study that the lowest propagation speed values was indeed found in the zero-stress state. This makes sense considering that the stress-strain properties of biological tissues are exponential-like [18] and that the propagation speed is proportional to the square root of the elastic modulus [13]. Releasing the residual stress causes the elastic moduli to decrease resulting in lowering of the propagation speed. The trend of increasing propagation speed with the loading level was most evident for the muscle tissue. The reason for the lesser response in the mucosa layer is likely that it is compressed in the no-load state and unfolds rather than stretches during low degrees of distension [2,18].

Comparable quantitative ultrasound data to the best of our knowledge have not been reported for the esophagus. However, values of propagation speed obtained from muscle in other organs [7,9,20] are similar to the ones found in the esophageal muscle coat in this study. In addition, the values for mucosa in this study agree with recent measurements in urethra [20,21] where it was also found that the propagation speed was highest in the muscle layer. The similarity with other tissues suggests that the freezing technique used in this study did not change the ultrasonic properties significantly. It was a principal result that the propagation speed was higher in the muscle layer than in mucosa of esophagus. The accuracy and error of SLAM for speed measurements have previously been estimated to be $\pm 2.9\%$ and $\pm 0.4\%$, respectively [7]. Hence, the difference in propagation speed between the muscle and mucosa layers cannot be explained by measurement uncertainties. It is well known that gastrointestinal mucosa–submucosa contains vessels, nerves, some muscle cells, and loose connective tissue. Only a part of the submucosa contains high amounts of collagen. The muscle tissue contains a high amount of actin–myosin proteins in the muscle cells and collagen fibers between the muscle cells. It is therefore not surprising that the highest propagation speed was found in the muscle layer since connective tissue fibers in other tissues have been shown to have a relatively high propagation speed [22]. Thus, the elastic stiffness will increase with the amount of collagen and the ultrasonic propagation speed will increase with collagen content since the speed is proportional to the square root of the elastic modulus of the material as shown by Fields et al. [23] and Goss and O'Brien [13]. Another contributing factor to the difference in propagation speed between the muscle and mucosa layers may be that the muscle layers are exposed to a higher tensile stress than the mucosa. According to a previous study on residual strains in the layered esophagus [2], it is evident that the mucosa–submucosa layer is compressed by the tension in the muscle layer at the no-load state, at low degrees of distension, and even at the zero-stress state if the muscle layer is not separated surgically from the mucosa–submucosal layer. We were not able to demonstrate differences in propagation speed between the two orthogonal muscle layers. This is in contrast to a previous study on bovine longissimus dorsi, psoas major and lobster extensor, where the speed was significantly higher for ultrasound parallel to the muscle fibers than perpendicular to the muscle fibers [24].

This study focused on the muscle and mucosa layers and showed differences between layers and loading states. Future studies should focus on ultrasonic properties in various directions in order to obtain more detailed data on tissue anisotropy and heterogeneity in the gastrointestinal tract.

Acknowledgements

This work is partially supported by a grant from The Danish Research Councils (9501709), Karen Elise Jensens Foundation, and the US National Institutes of Health (CA09067). The authors acknowledge the help from James F. Zachary, DVM, Ph.D., Veterinary Pathobiology, and Ann C. Benefiel, Biological Resources, Beckman Institute for Advanced Science and Technology, both at the University of Illinois.

References

[1] R. Yu, J. Zhon, Y.C. Fung, Neutral axis location in bending and Young's modulus of different layers of arterial wall, Am. J. Physiol. 265 (1993) H52–H60.
[2] H. Gregersen, C. Lee, S. Chien, R. Skalak, Y.C. Fung, Strain distribution in the layered wall of the esophagus, J. Biomech. Engng. 121 (1999) 442–448.
[3] F.V. Hunt, Origins of Acoustics New Haven, Yale University Press, New Haven, CT 1978.
[4] G. Wade, Acoustic Imaging, Plenum Press, New York, 1976.
[5] A. Korpel, L.W. Kessler, P.R. Palermo, Acoustic microscope operating 100 MHz, Nature 232 (1971) 110–111.
[6] J.A. Slobin, D.L. Stocum, W.D. O'Brien Jr., Amphibian limb regeneration curves generated by the scanning laser acoustic microscope, J. Histochem. Cytochem. 34 (1986) 53–56.
[7] D.L. Steiger, W.D. O'Brien Jr., J.E. Olerud, M.A. Riederer-Henderson, G.F. Odland, Measurement uncertainty assessment of the scanning laser acoustic microscope and application to canine skin and wound, IEEE Trans. Ultra Ferroelec. Freq. Contrl. 35 (1988) 741–748.
[8] L.W. Kessler, S.I. Fields, F. Dunn, Acoustic microscope of mammalian kidney, J. Clin. Ultrasound 2 (1974) 317–320.
[9] K.M.U. Tervola, M.A. Gummer, J.W. Erdman Jr., W.D. O'Brien Jr., Ultrasound attenuation and velocities in rat liver as a function of fat concentration: a study at 100 MHz using a scanning laser acoustic microscope, J. Acoust. Soc. Am. 77 (1985) 307–313.
[10] L.W. Kessler, A. Korpel, P.R. Palermo, Simultaneous acoustic and optical microscopy of biological specimens, Nature 239 (1972) 111–112.
[11] K.M.U. Tervola, S.G. Foster, W.D. O'Brien Jr., Attenuation coefficient measurement technique at 100 MHz with the scanning laser acoustic microscope, IEEE Trans. Sonics Ultrason. SU-32 (1985) 259–265.
[12] K.M.U. Tervola, W.D. O'Brien Jr., Spatial frequency domain technique: an approach for analyzing the scanning laser acoustic microscope interferogram images, IEEE Trans. Sonics Ultrason. 4 (1985) 544–554.
[13] S.A. Goss, W.D. O'Brien Jr., Direct ultrasonic velocity measurements of mammalian collagen threads, J. Acoust. Soc. Am. 65 (2) (1979) 507–511.
[14] F. Dunn, P.D. Edmonds, W.J. Fry, Absorption and dispersion of ultrasound in biological media, in: H.P. Schwan (Ed.), Biological Engineering, McGraw Hill, New York, 1969.
[15] B. Zeqiri, Reference liquid for ultrasonic attenuation, Ultrasonics 27 (1989) 314–315.
[16] Y.C. Fung, What principle governs the stress distribution in living organs? in: Y.C. Fung, E. Fukuda, W. Junjian (Ed.), Biomechanics in China, Japan and USA, Science, Beijing, 1983.
[17] R.N. Vaishnav, J. Vossoughi, Estimation of residual strain in aortic segments, in: C.W. Hall (Ed.), Biomedical Engineering. II. Recent Developments. Pergamon Press, New York, 1983, pp. 330–333.
[18] H. Gregersen, G.S. Kassab, Biomechanics of the gastrointestinal tract, Neurogastroent. Motil. 8 (1996) 277–297.
[19] H. Gregersen, G.S. Kassab, E. Pallencaoe, C. Lee, S. Chien, R. Skalak, Y.C. Fung, Morphometry and strain distribution in guinea pig duodenum with reference to the zero-stress state, Am. J. Physiol. 273 (1997) G865–G874.
[20] J.E. Assentoft, C.S. Jørgensen, H. Gregersen, L.L. Christensen, J.C. Djurhuus, W.D. O'Brien Jr., Characterizing biological tissue using scanning laser acoustic microscopy, IEEE Engng. Med. Biol. 15 (1996) 42–45.
[21] C.R. Hill (Ed.), Physical Principles of Medical Ultrasonics, Wiley, New York, 1986.
[22] C.A. Edwards, W.D. O'Brien Jr., Speed of sound in mammalian tendon threads using various reference media, IEEE Trans. Sonics Ultrason. SU32 (1985) 351–354.
[23] S. Fields, F. Dunn, Correlation of echographic visualization of tissue with biological composition and physiological state, J. Acoust. Soc. Am. 54 (1973) 809–812.
[24] N.B. Smith, Effect of myofibril length and tissue constituents on acoustic propagation properties of muscle, Ph.D. Thesis, University of Illinois at Urbana-Champaign, 1996.